PROCEEDINGS OF SCIENCE

Charm physics by $N_f = 2+1$ Iwasaki gauge and the six stout smeared $O(a)$-improved Wilson quark actions on a 96^4 lattice

Y.Namekawa* **for PACS Collaboration**
Center for Computational Sciences, University of Tsukuba, Tsukuba, Ibaraki 305-8577, Japan
E-mail: namekawa@ccs.tsukuba.ac.jp

Our results of charm physics in $N_f = 2+1$ lattice QCD are presented. The calculation is performed on configurations generated using Iwasaki gauge and six stout smeared $O(a)$-improved Wilson quark actions with the smearing parameter $\rho = 0.1$ on a 96^4 lattice at $\beta = 1.82$ ($a^{-1} = 2.3$ GeV) with the spatial extent $L = 8.1$ fm. The pion mass at the simulation point is almost physical, $m_\pi = 146$ MeV, extrapolated to the physical point by use of reweighting. The relativistic heavy quark action is utilized for the charm quark. We exhibit the charmed spectrum and the charm quark mass, focusing on stout smearing influence.

34th annual International Symposium on Lattice Field Theory
24-30 July 2016
University of Southampton, UK

*Speaker.

PoS(LATTICE2016)125

1. Introduction

Lattice QCD is a robust tool for charm physics. A number of simulations are performed to investigate the charm quark system non-perturbatively. Recent results by lattice QCD are summarized by FLAG Working Group [1]. A lattice calculation for the charm quark needs control of large cutoff errors due to the charm quark mass, which is $m_{\rm charm}a \sim 0.4$ at a typical lattice spacing of $a^{-1} = 2$ GeV. Conventional lattice quark actions as well as heavy quark improved actions are adopted for a charm quark on the lattice. Our choice is the relativistic heavy quark action of Ref. [2]. This action is formulated to reduce heavy quark mass corrections of $O((m_Q a)^n)$ with arbitrary order n to $O(f(m_Q a)(a\Lambda_{QCD})^2)$, where $f(m_Q a)$ is an analytic function around the massless point $m_Q a = 0$.

In our previous works [3, 4], simulations of the charm quark system are accomplished on the physical point. Uncertainty from the chiral extrapolation is completely removed. There are, however, still two remaining major sources of systematic errors. One is the discretization error. It is reduced by the improved action, and shall vanish in the continuum limit. We are generating gauge configurations with lattice spacings down to 3 GeV to complete a continuum extrapolation. The other is the finite size effect. Although it is small for charmed hadrons due to a large mass of the charm quark, an indirect finite size effect can appear through determination of the physical point. The physical point is defined by masses of π, K mesons and Ω baryon. Finite size effects to these masses shift an estimated value of the physical point.

PACS Collaboration performs a large spatial volume simulation on a 96^4 lattice near the physical point with the pion mass $m_\pi = 146$ MeV [5]. The spatial size is $L = 8.1$ fm, $m_\pi L = 6$, in which the finite size effect is suppressed enormously. Our results for charm physics on this lattice are reported.

2. Simulation parameters

Measurement of the charm quantities is carried out with the relativistic heavy quark action of Ref. [2] on the 2+1 flavor lattice QCD configurations generated by the PACS Collaboration [5]. The nonperturbatively $O(a)$-improved Wilson quark action with $c_{\rm SW}^{\rm NP} = 1.11$ is employed using six stout smearing with the smearing parameter $\rho = 0.1$ [6, 7]. The gauge action is Iwasaki type [8]. The lattice size is $96^3 \times 96$ with the lattice spacing of $a^{-1} = 2.33(2)$ GeV at $\beta = 1.82$. The dynamical up-down and strange quark masses at the simulation point are close to their physical values, corresponding to the pion mass $m_\pi = 146$ MeV. A short chiral extrapolation is performed adopting a reweighting technique for production of data around the simulation point. The value at the physical point is obtained by fitting these reweighted data. The number of configurations is 200, corresponding to 2000 MD time. Our statistical errors are analyzed by the Jackknife procedure with a bin size of 50 traj.

The relativistic heavy quark action is given by

$$S_Q = \sum_{x,y} \overline{Q}_x D_{x,y} Q_y, \tag{2.1}$$

$$
\begin{aligned}
D_{x,y} \;=\; & \delta_{xy} - \kappa_{\rm h} \sum_i \Big[(r_s - \nu\gamma_i) U_{x,i} \delta_{x+\hat{i},y} + (r_s + \nu\gamma_i) U^\dagger_{x,i} \delta_{x,y+\hat{i}} \Big] \\
& - \kappa_{\rm h} \Big[(1 - \nu\gamma_i) U_{x,4} \delta_{x+\hat{4},y} + (1 + \nu\gamma_i) U^\dagger_{x,4} \delta_{x,y+\hat{4}} \Big] \\
& - \kappa_{\rm h} \left[c_B \sum_{i,j} F_{ij}(x) \sigma_{ij} + c_E \sum_i F_{i4}(x) \sigma_{i4} \right], \qquad (2.2)
\end{aligned}
$$

where $\kappa_{\rm h}$ is a hopping parameter of the heavy quark Q. The four parameters ν, r_s, c_B, c_E are calibrated in a mass dependent way. The one-loop perturbative values are used for r_s, c_B and c_E [9]. In contrast to our previous works [3, 4], no tadpole improvement is adopted. Our plaquette value is close to one, plaq=0.97, which suggests the tadpole contribution is almost eliminated by the stout smearing of the gauge link. For the clover coefficients c_B and c_E the nonperturbative contributions are included in part by $c_{B,E} = (c_{B,E}(m_Q a) - c_{B,E}(0))^{\rm PT} + c^{\rm NP}_{\rm SW}$, where $c^{\rm NP}_{\rm SW} = 1.11$ is the value at the massless limit. The parameter ν is nonperturbatively determined from the dispersion relation for the spin-averaged $1S$ state of the charmonium, $E(\vec{p})^2 = E(\vec{0})^2 + c^2_{\rm eff}|\vec{p}|^2$. ν is adjusted such that the effective speed of light $c_{\rm eff}$ becomes unity.

Figure 1 represents the dispersion relation and the effective speed of light. The large spatial volume 96^3 provides fine resolution for momentum. The effective speed of light can be determined with high precision. The effective speed of light with a perturbative choice of ν is close to one by the heavy quark action improvement, but slightly underestimated by 4%. Non-perturbative tuning of ν realizes $c^{\rm 1S}_{\rm eff} = 1$, as plotted in Fig.2.

Charmonium masses are calculated using standard operators defined by $M_\Gamma(x) = \bar{Q}(x)\Gamma Q(x)$, where $\Gamma = I, \gamma_5, \gamma_\mu, i\gamma_\mu\gamma_5, i[\gamma_\mu, \gamma_\nu]/2$. Point and wall sources as well as a local sink are utilized for them. The number of source points is four, and polarizations are averaged to lessen the statistical fluctuations. The physical point of the charm quark is identified by the condition that the mass of the spin-averaged $1S$ state reproduces the experimental value, $M^{\rm exp}(1S) = (M^{\rm exp}_{\eta_c} + 3M^{\rm exp}_{J/\psi})/4 = 3.0685(1)$ GeV [11]. Two values of $\kappa_{\rm h}$ are chosen to interpose the physical charm quark mass, as compiled in Table 1.

It is noted the stopping condition $\varepsilon > |Dx - b|/|b|$ must be strict for a calculation of the charm quark propagator [10]. A result with a loose stopping condition deviates from the strict value, where the correlation function has a tiny value comparable with the stopping condition squared. In this work, $\varepsilon = 10^{-14}$ is set for inversions of the charm quark matrix.

3. Result

Charmonium masses are extracted by fitting the correlators with a hyperbolic cosine function. The fitting range is $[t_{\rm min}, t_{\rm max}] = [30, 35]$ for pseudoscalar and vector mesons, and $[t_{\rm min}, t_{\rm max}] = [20, 25]$ for others channels. Data in a large t region are not used for our analysis, where rounding errors can be sizable in comparison with the statistical errors.

Measured masses of charmonium are extrapolated to the physical point by a linear function of the up-down and the strange quark masses normalized by Ω baryon mass, which defines the lattice spacing,

$$
(m/m_\Omega) M^{\rm exp}_\Omega = A + B(m_{\rm ud} - m^{\rm phys}_{\rm ud}) + C(m_{\rm s} - m^{\rm phys}_{\rm s}), \qquad (3.1)
$$

Table 1: Simulation parameters. $(\kappa_{ud}, \kappa_s) = (0.126117, 0.124790)$ is the simulation point, while the others are reweighted points.

κ_{ud}	κ_s	κ_h
0.126111	0.124790	0.098405, 0.099017
0.126111	0.124812	0.098405, 0.099017
0.126111	0.124824	0.098405, 0.099017
0.126111	0.124834	0.098405, 0.099017
0.126117	0.124768	0.098405, 0.099017
0.126117	0.124790	0.098405, 0.099017
0.126117	0.124812	0.098405, 0.099017

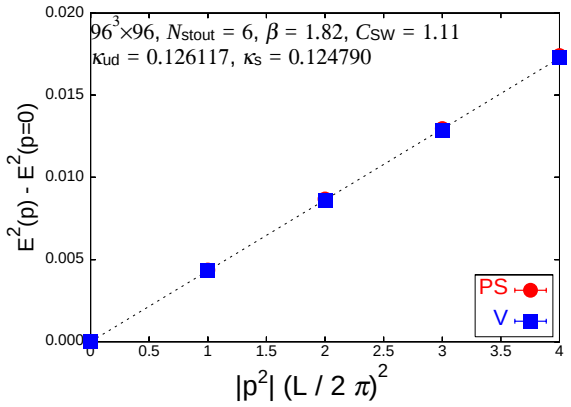

Figure 1: Dispersion relation of a charmonium in pseudoscalar and vector channels.

where A, B, C are fitting parameters, and $M_\Omega^{\rm exp} = 1.6725(3)$ GeV [11]. Since our simulation is performed near the physical point, $\max|m_{ud} - m_{ud}^{\rm phys}| = 1$ MeV and $\max|m_s - m_s^{\rm phys}| = 10$ MeV, higher order corrections are expected to be diminutive. In fact, little dynamical quark mass dependence is observed for the charmonium spectrum within the range of our quark masses. Fig. 3 exhibits our results for the charmonium mass spectrum. They are consistent with the experimental values within the error, except for the hyperfine splitting.

Figure 4 focuses on the hyperfine splitting $m_{J/\psi} - m_{\eta_c}$. The extrapolated result shows a 14% deficit from the experimental value. Gauge link smearing does not shrink the difference between our lattice result and the experimental value of the hyperfine splitting. The main source of the discrepancy must be a discretization effect. The continuum limit is needed to draw a definitive estimation.

The charm quark mass is obtained by the axial Ward-Takahashi identity, $m_{\rm charm}^{\rm AWI} = \frac{m_{\rm PS}}{2} \frac{\langle 0|A_4^{\rm imp}|PS\rangle}{\langle 0|P|PS\rangle}$, where P is the pseudoscalar meson operator, and $A_4^{\rm imp}$ is the improved axial vector current defined by $A_4^{\rm imp} = \bar{Q}(x)\gamma_4\gamma_5 Q(x) + c_{A_4}^+ \partial_4^+ \left(\bar{Q}(x)\gamma_5 Q(x)\right)$. A perturbative value is set for the improvement coefficient of the axial vector current $c_{A_4}^+$ [12]. In contrast to $C_{\rm SW}$ case, non-perturbative contribution at the massless limit is not included for $c_{A_4}^+$, as is found to be consistent with zero. The renormal-

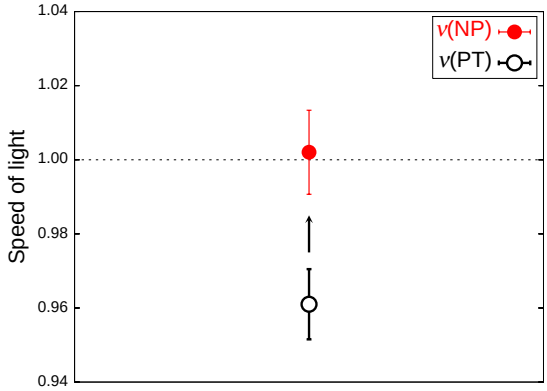

Figure 2: Effective speed of light for the spin-averaged 1S state of the charmonium with a perturbative and nonperturbative choice of the action parameter ν.

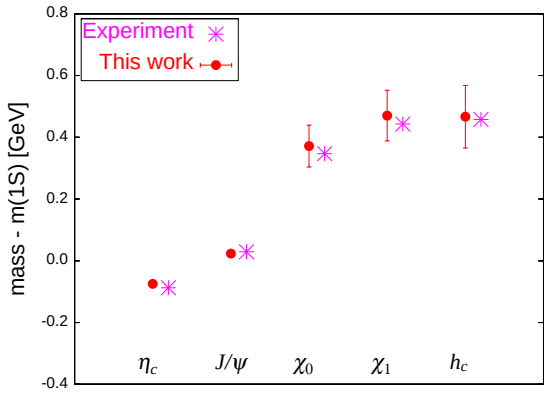

Figure 3: Charmonium spectrum.

ized charm quark mass in the $\overline{\rm MS}$ scheme is given by $m^{\overline{\rm MS}}_{\rm charm}(\mu) = Z_m(\mu) m^{\rm AWI}_{\rm charm}$. The renormalization factor consists of a perturbative estimate [12], combined with the non-perturbative value at the massless point, $Z_{\rm m}(\mu) = (Z_{\rm m}(\mu, m_Q a) - Z_{\rm m}(\mu, 0))^{\rm PT} + Z_{\rm m}(\mu)^{\rm NP}$, where $Z^{\rm NP}_{\rm m}(\mu = 2{\rm GeV}) = 0.995(14)$ [13]. It is noticed that the stout smearing is efficient in reducing uncertainty of the renormalization factor, which is a major source of the systematic errors of the charm quark mass. The renormalized charm quark mass is evolved to $\mu = m^{\overline{\rm MS}}_{\rm charm}$ by four-loop beta function [14]. Fig. 5 collates the results of the charm quark. As in the case of light quark masses [5], our result has a smaller value than the FLAG average [1]. A finite lattice spacing seems to cause the discrepancy. The right panel of Fig. 5 explains the charm quark mass normalized by the strange quark mass. The discretization error is reduced in a ratio of quark masses. The deviation from the FLAG value decreases.

4. Conclusion

Our results of charmed quantities are reported. The measurement is executed near the physical

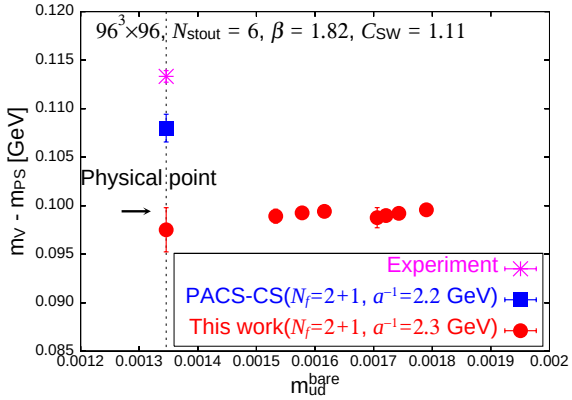

Figure 4: Hyperfine splitting of the charmonium as a function of $m_{\rm ud}^{\rm AWI}$. A vertical dotted line denotes the physical point.

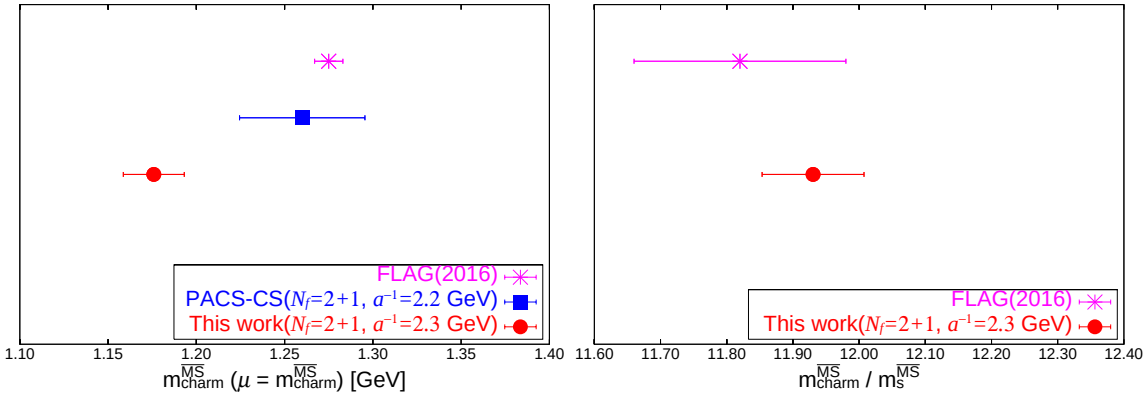

Figure 5: Charm quark mass (left panel), and mass ratio of the charm quark to the strange quark (right panel).

point at $a^{-1} = 2.3$ GeV with a spatial extent $L = 8.1$ fm, $m_\pi L = 6$, using six stout smeared $O(a)$-improved Wilson quark action with the smearing parameter $\rho = 0.1$ and Iwasaki gauge action in $N_f = 2+1$ QCD. The relativistic heavy quark action of Ref. [2] is applied to the charm quark. The large spatial volume yields insignificant finite size effects to not only charmed hadrons but also light hadrons which define the physical point.

The charmonium spectrum obtained in our calculation agrees with experiments, except for the hyperfine splitting. Our hyperfine splitting underestimated the experimental value, as in our previous work at $a^{-1} = 2.2$ GeV with no stout smearing [3]. It indicates the stout smearing is not profitable to reduce a lattice artifact in the hyperfine splitting. For comprehensive evaluation of the stout smearing, other measurements such as the heavy-light system, form factors are performed. In contrast, the stout smearing shows an advantage in a computation of the charm quark mass. The uncertainty of the renormalization factor is reduced. Our result of the charm quark mass deviates from the FLAG average, but the difference decreases significantly in the quark mass ratio. It suggests the deviation is caused by a finite lattice spacing. The remaining task is the continuum

extrapolation. The continuum limit will be achieved employing gauge configurations at finer lattice spacings, which are under generation.

Acknowledgments

The numerical calculations were carried out on XC40 at YITP in Kyoto University. This work is in part based on Bridge++ code [15]. This work is supported in part by Grants-in-Aid for Scientific Research from the Ministry of Education, Culture, Sports, Science and Technology (No.15K05068).

References

[1] FLAG Working Group, S. Aoki *et al.*, arXiv:1607.00299

[2] S. Aoki, Y. Kuramashi and S. Tominaga, Prog. Theor. Phys. 109 (2003) 383

[3] PACS-CS Collaboration, Y. Namekawa *et al.*, Phys. Rev. D84 (2011) 074505

[4] PACS-CS Collaboration, Y. Namekawa *et al.*, Phys. Rev. D87 (2013) 094512

[5] PACS-CS Collaboration, K-I.Ishikawa *et al.*, PoS(LATTICE 2015) (2016) 075

[6] C. Morningstar and M. J. Peardon, Phys. Rev. D69 (2004) 054501

[7] BMW Collaboration, S. Dürr *et al.*, Phys. Rev. D79 (2009) 014501

[8] Y. Iwasaki, UTHEP-118 (1983); arXiv:1111.7054

[9] S. Aoki, Y. Kayaba and Y. Kuramashi, Nucl. Phys. B697 (2004) 271

[10] See e.g. A. Jüttner and M. D. Morte, PoS(LATTICE 2005) (2005) 204

[11] Particle Data Group, C. Patrignani *et al.*, Chin. Phys. C40 (2016)

[12] S. Aoki, Y. Kayaba and Y. Kuramashi, Nucl. Phys. B689 (2004) 127

[13] PACS-CS Collaboration, K-I.Ishikawa *et al.*, PoS(LATTICE 2015) (2016) 271

[14] K.G. Chetyrkin, Phys. Lett. B404 (1997) 161; J.A.M. Vermaseren *et al.*, Phys. Lett. B405 (1997) 327

[15] http://bridge.kek.jp/Lattice-code/